

Spatial separation of 2-propanol monomer and its ionization-fragmentation pathways

Jia Wang,^{1,||} Lanhai He,^{1,§} Jovana Petrovic,¹ Ahmed Al-Refaie,^{1,‡}
Helen Bieker,^{1,2} Jolijn Onvlee,^{1,3} Karol Długołęcki,¹ and Jochen Küpper^{1,2,3,*}

¹Center for Free-Electron Laser Science, Deutsches Elektronen-Synchrotron DESY, Notkestraße 85, 22607 Hamburg, Germany

²Department of Physics, Universität Hamburg, Luruper Chaussee 149, 22761 Hamburg, Germany

³Center for Ultrafast Imaging, Universität Hamburg, Luruper Chaussee 149, 22761 Hamburg, Germany

The spatial separation of 2-propanol monomer from its clusters in a molecular beam by an electrostatic deflector was demonstrated. Samples of 2-propanol monomer with a purity of 90 % and a beam density of $7 \times 10^6 \text{ cm}^{-3}$ were obtained. These samples were utilized to study the femtosecond-laser-induced strong-field multi-photon ionization and fragmentation of 2-propanol using non-resonant 800 nm light with peak intensities of $3\text{--}7 \times 10^{13} \text{ W/cm}^2$.

Dedicated to the legacy of Jon T. Hougen.[†]

INTRODUCTION

2-propanol ($\text{C}_3\text{H}_8\text{O}$, also isopropyl alcohol, isopropanol) is the simplest secondary alcohol. It possesses a structure with three nonrigid internal rotations, i. e., of the hydroxyl group OH and two methyl tops CH_3 [1–3]. 2-propanol has attracted much attention, not only because it is highly valued as a preservative and used as an antiseptic in the clinical environment, but also since it is widely used as an industrial solvent and cleaning fluid, such as gasoline additive, an alkylating agent, and a disinfectant [4, 5]. The vibrational spectrum of 2-propanol has been studied in the early 1960s, which suggested that 2-propanol in the gas phase exists in trans and gauche conformations [6]. These stable isomers were confirmed by the microwave [7–10] and the millimeter- and submillimeter-wave spectra [3, 5].

Supersonic molecular beams are a valuable tool for molecular spectroscopy and the studies of molecular dynamics and reactions [11–13]. For instance, this was exploited in studies of the hydrogen bonding in 2-propanol [14] and its hydrogen-bonded complexes [15, 16]. Generally, the supersonic expansion provides beams of molecular at low rotational temperatures. However, clusters can be formed [11, 12, 17] due to the attractive forces between molecules. The temperature- and pressure-dependence of its cluster formation was investigated [18, 19]. Other factors influencing the cluster formation in expanding supersonic jets are the nozzle size and shape and the carrier gas [11, 20, 21]. Larger clusters are often fragile and then fragment upon excitation or ionization before detection, rendering size-assignment from spectra ambiguous or even impossible [22, 23].

For prospective studies of 2-propanol in chemical-reactions [24, 25] or diffractive-imaging experiments [26, 27], a cold and pure beam of 2-propanol separated from clusters as well as seed gas is necessary [28, 29]. Such spatial separation of molecular conformers was previously achieved using inhomogeneous electric fields [29, 30]. Different species of complex molecules can be spatially separated within a cold molecular beam by the electrostatic

deflector [29], which was demonstrated in a number of pioneering experiments on the separation of individual quantum states [31–33], structural isomers [34, 35], or specific cluster sizes [36–40]. Here, the 2-propanol monomer is spatially separated from the original molecular beam using the deflector and the purified samples are exploited in femtosecond-laser ionization studies.

EXPERIMENTAL METHODS

2-propanol was commercially obtained (Carl Roth GmbH, > 99 %) and used without further purification. Fig. 1 shows a schematic of the experimental setup, similar to a previously described one [37]. Briefly, 2-propanol at room temperature is seeded in 2 bar of helium and supersonically expanded into vacuum through a cantilever piezo valve [41] at a repetition rate of 20 Hz. The produced molecular beam was differentially pumped and collimated by two skimmers, which were placed 55 mm ($\varnothing = 3 \text{ mm}$) and 365 mm ($\varnothing = 1.5 \text{ mm}$) downstream of the valve, and directed through the electrostatic deflector,

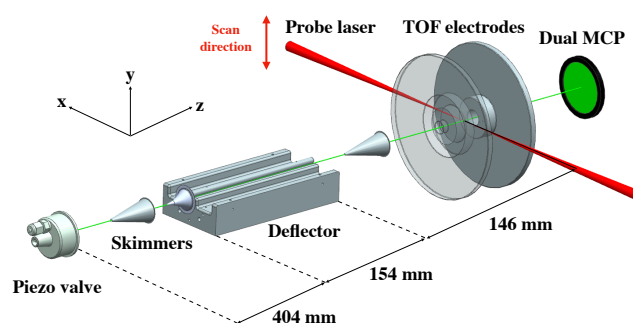


FIG. 1. Schematic of the experimental setup. It includes a piezo valve, the electrostatic deflector, a femtosecond laser, and a two-plate electrode and time-of-flight (TOF) mass spectrometer; see text for details.

before passing through a third skimmer ($\varnothing = 1.5$ mm). 2-propanol molecules were ionized by amplified femtosecond laser pulses with a duration of 45 fs (full-width at half maximum, FWHM) with a spectrum centered around 800 nm. By focusing the laser with pulse energies of 30 μ J and 60 μ J to 50 μ m, we obtained nominal peak intensities of 3×10^{13} W/cm² and 7×10^{13} W/cm², respectively. A two-plate VMI [42] was operated as a time-of-flight (TOF) mass spectrometer (MS). Ions were counted through a single-shot detector readout and centroiding algorithm [43], and summed up to yield the mass spectra shown in Fig. 2 a, b.

RESULTS AND DISCUSSION

The mass spectra at peak intensities of 3×10^{13} W/cm² and 7×10^{13} W/cm² of the direct (0 kV) and deflected (13 kV) molecular beams are shown in Fig. 2. The spectrum of the direct beam shows 2-propanol fragment ions ($[\text{M-OH}]^+$ and $[\text{M-CH}_3]^+$), monomer ions M^+ , and protonated 2-propanol and its cluster ions $[\text{M}_n+\text{H}]^+$ up to $n = 5$. The mass spectra in Fig. 2 a and Fig. 2 b were normalized to their largest peak. Larger clusters were not detected due to the recorded TOF interval in the experiments. Note that the clusters of 2-propanol in the interaction region are neutral and that the protonated-cluster ions in the mass spectrum resulted from the ionization detection process [39, 40].

The spatial vertical molecular-beam-density profiles for 2-propanol monomer ions, fragment ions, protonated 2-propanol, and its cluster ions $[\text{M}_n+\text{H}]^+$ up to $n = 5$, ionized with the laser peak intensities of 3×10^{13} W/cm² and 7×10^{13} W/cm², are shown in Fig. 2 c and Fig. 2 d. The direct and deflected profiles were normalized to their largest signals. For better visibility, the M^+ deflection profile has been scaled up by a factor of 5.5. When a voltage of 13 kV is applied to the deflector, the profiles of fragment ions ($[\text{M-OH}]^+$ and $[\text{M-CH}_3]^+$), and the parent ion M^+ are shifted by +1.8 mm at both laser peak intensities; the $[\text{2M-CH}_3]^+$ profile also has a tail with significant deflection, which we ascribe to a fairly polar cluster, but this species deflects less and has only a small population in the beam. The protonated 2-propanol and its cluster ions in Fig. 2 c and Fig. 2 d do not deflect in the region of 1.1 to 1.8 mm, which shows that dimers and larger clusters generally deflect much less than the monomer and the monomer ion signal originated from the monomer.

2-propanol is a nearly symmetric oblate rotor, the rotational constants for *trans* and *gauche* were obtained by microwave spectroscopy [8]. The dipole-moment components are $\mu_a = 0, \mu_b = 1.40$ D, $\mu_c = 0.73$ D for the *trans* [7] and $\mu_a = 1.114$ D, $\mu_b = 0.737$ D, $\mu_c = 0.813$ D for the *gauche* conformer, respectively [8]. Their energy difference is smaller than 1 kJ/mol and the isomerization barrier corresponding to rotation of the hydroxyl moiety

is low [16]. The *gauche* conformer is more stable than the *trans* conformer and there is a strong conformational relaxation of 2-propanol monomer from *trans* to *gauche* [44]. Using the specified dipole-moment components and the known rotational constants [8], the Stark energies and effective dipole moments of both forms were calculated with our CMISTARK software package [45]. The Stark-effect differences between the two conformers are too small for their separation in this experiment. Furthermore, it is difficult to determine the ratio between the *trans* and *gauche* forms at low temperatures as they are essentially identical. For the analysis in this work, we used only the *trans*-conformer deflection simulations.

The simulated vertical molecular-beam profiles of the 2-propanol monomer are shown in Fig. 2 c and Fig. 2 d. The Stark energies for all rotational states up to $J = 14$, including all states up to $J = 30$ in the calculation, were calculated. For every quantum state, 1×10^5 trajectories were calculated. The initial beam temperature that described the experimental observations best was determined to be 3.5(5) K. The shaded (dark red) area depicts the error estimate of the 2-propanol simulation due to the temperature uncertainty.

In Fig. 2 c the deflected profiles (dashed lines) of monomer (red squares) and $[\text{M-CH}_3]^+$ ions (black squares) matched very well over the whole deflection region, indicating that $[\text{M-CH}_3]^+$ and M^+ both originated from the parent molecule. However, at higher peak ionization-laser intensity, Fig. 2 d, the profiles of monomer and $[\text{M-CH}_3]^+$ ions matched only in the region of 1.1 to 1.8 mm. The higher $[\text{M-CH}_3]^+$ signal in the [-1,1] regions indicates the contribution of larger clusters to this fragment in the ion signals. Nevertheless, this behavior nicely confirms the selection of monomers from the expansion in the deflected part at positions larger than 1.1 mm.

The deflected-beam mass spectra in Fig. 2 a and Fig. 2 b mainly contained peaks corresponding to $[\text{M-OH}]^+$, $[\text{M-CH}_3]^+$, M^+ and $[\text{2M-CH}_3]^+$ at both laser peak intensities. The fragments were caused by the fs-pulse ionization process, however, no hydrogen ions were observed in the TOF spectrum in Fig. 2 a due to the low laser peak intensity. The ratios of different fragments and M^+ ions from the center position to 1.6 mm are shown in Fig. 3. For both laser peak intensities, the ratios for $[\text{M-OH}]^+$, and $[\text{M-CH}_3]^+$ ions in the deflected region from 1.1 mm to 1.6 mm are constant, which suggests $[\text{M-OH}]^+$, $[\text{M-CH}_3]^+$ and M^+ ions come from the same parent, the monomer. However, the ratio for $[\text{2M-CH}_3]^+$ decreases as the position increases in Fig. 3 a and Fig. 3 b, indicating that this peak originates from the dimer or larger clusters, which are deflected out of the original beam, but less than the monomer.

Following the strong-field/multi-photon ionization process of 2-propanol, C-C and C-O bonds of the monomer were broken. This suggests that the monomer has two fragmentation channels, $\text{M} \rightarrow [\text{M-CH}_3]^+$ and $\text{M} \rightarrow [\text{M-}$

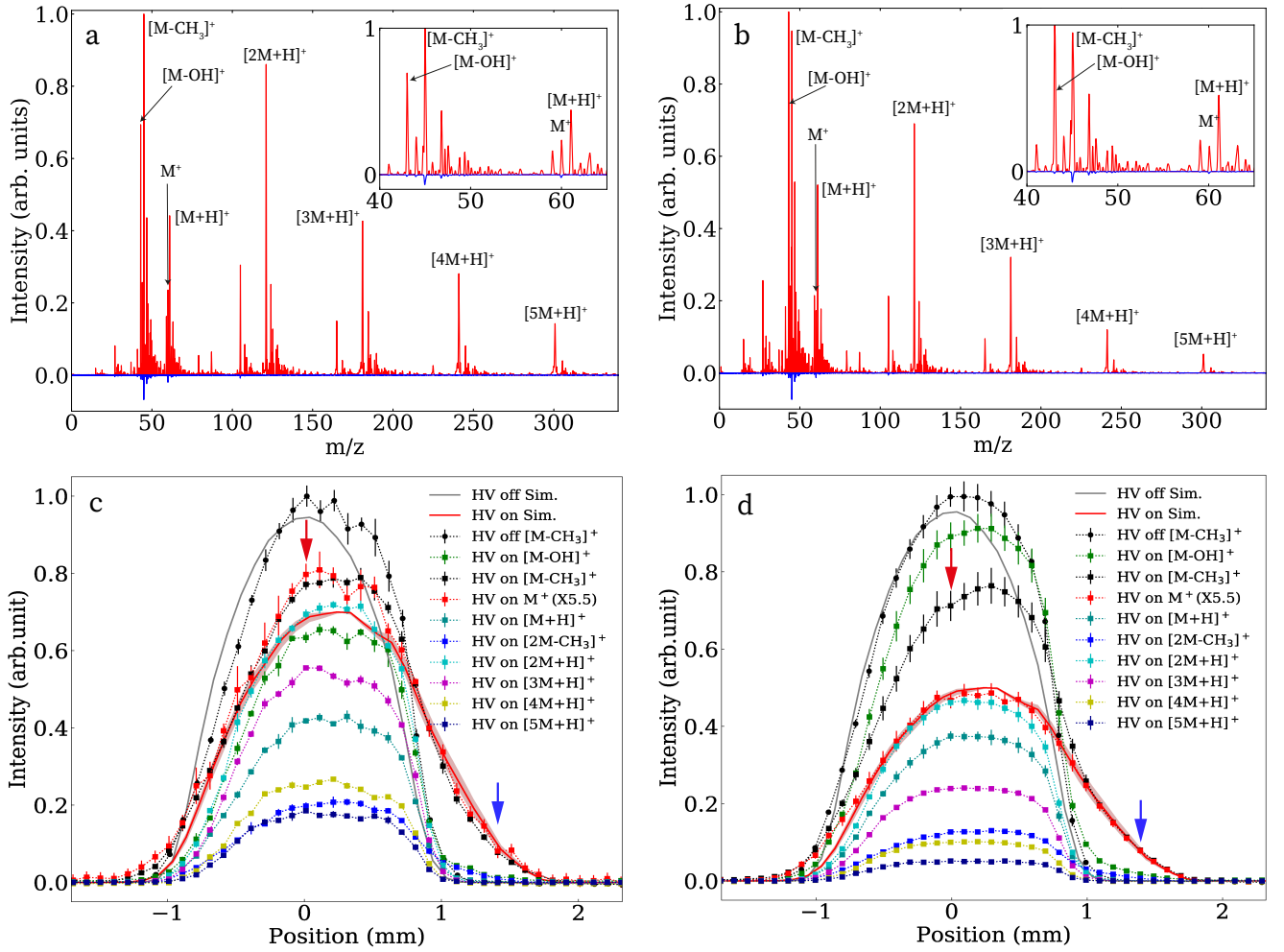


FIG. 2. Mass spectra and vertical molecular-beam-density profiles with peak intensities of (a, c) 3×10^{13} W/cm² and (b, d) 7×10^{13} W/cm². (a) and (b) TOF-MS in the central part of the molecular beam without a deflection voltage (red) and at a position of +1.4 mm with a deflection voltage of 13 kV (blue) as depicted in the panels below. (c) and (d) 0 kV (circle) and 13 kV (square) vertical spatial-beam-profiles for both pulse energies. In the legends M refers to the monomer. Dashed lines show fragment cations of 2-propanol ($[M-OH]^+$ (green), $[M-CH_3]^+$ (black), $[2M-CH_3]^+$ (blue)), monomer cation M^+ (red), protonated 2-propanol $[M+H]^+$ (darkcyan) and its clusters up to $n = 5$ ($[2M+H]^+$ (cyan), $[3M+H]^+$ (magenta), $[4M+H]^+$ (yellow), $[5M+H]^+$ (darkblue)). Simulated deflection profiles of the direct 2-propanol monomer beam (grey circle) as well as the deflected 2-propanol monomer beam (red square) area are shown as solid lines. The shaded (dark red) area depicts the error estimate of the 2-propanol simulation due to the temperature uncertainty. The red and blue arrows indicate the positions in the deflected beam where the mass spectra shown in (a) and (b) were measured.

$OH]^+$.

Based on the intensity of the fragments of the 2-propanol in the deflected beam, Fig. 2 a and Fig. 2 b, the purity of the intact 2-propanol monomer was derived as the ratio of the sum of the signals due to M^+ and its known fragments $[M-OH]^+$ and $[M-CH_3]^+$ to the sum of all signals in the mass spectrum. The 2-propanol monomer fraction was 4(1) % in the center of the direct beam and 90(4) % at +1.4 mm in the deflected beam. This is a nearly 22-fold increase in the fractional density of 2-propanol from the direct beam to the deflected beam.

By comparing the intensities of $[M-CH_3]^+$ and $[M-OH]^+$

in Fig. 3 a and Fig. 3 b, the intensity ratio of the $M \rightarrow [M-CH_3]^+$ channel to the $M \rightarrow [M-OH]^+$ channel was obtained as ~ 5 for both peak intensities in the region from 1.1 mm to 1.6 mm. The fragmentation ratios of the monomer, defined as the intensities of the fragments divided by the sum of intensities of the monomer and its related fragments, were estimated as 83 % and 89 % at the lower and higher peak intensity, respectively.

The beam density was estimated based on the analog detector current signal calibrated to a single-ion hit. Approximately 7 ions/shot were created in the deflected beam (+1.4 mm) at a laser peak intensities of 7×10^{13} W/cm².

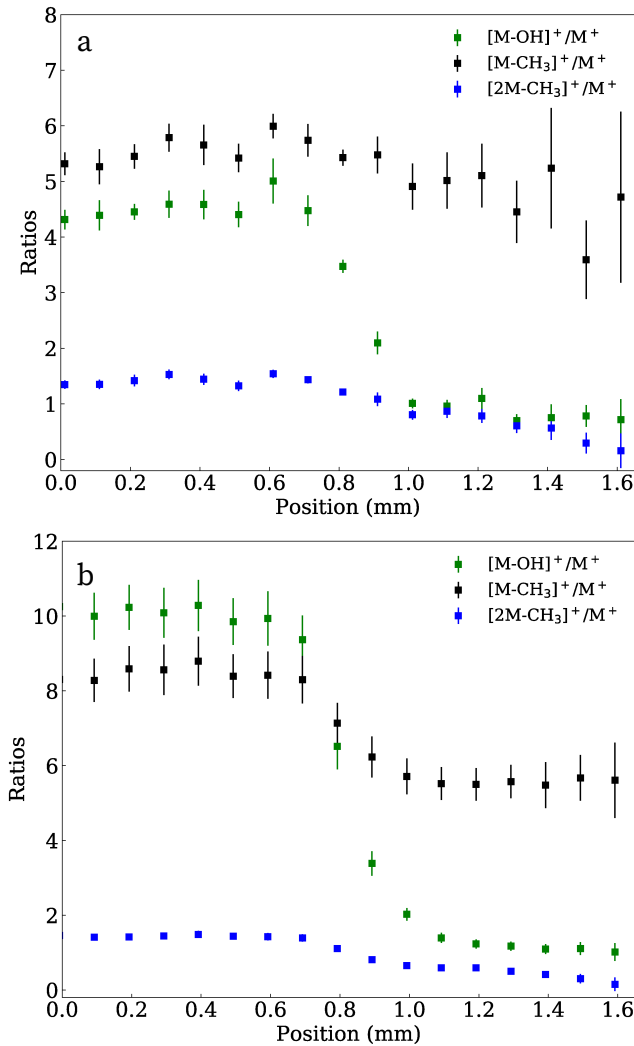


FIG. 3. The ratios of different fragment ions $[M-OH]^+$ (green), $[M-CH_3]^+$ (black), $[2M-CH_3]^+$ (blue) and M^+ ion in the deflected region with peak intensities of (a) 3×10^{13} W/cm² and (b) 7×10^{13} W/cm².

Assuming a typical detection efficiency of 0.5 for the MCP detector, a molecular-beam width of 1 mm, and a strong-field-ionization probability of 1, a beam density of $\sim 7 \times 10^6$ cm⁻³ was obtained for the 2-propanol monomer.

CONCLUSIONS

A high-purity beam of 2-propanol monomer was produced through the spatial separation of the monomer from its clusters and the seed gas using the electrostatic deflector. The purity and beam density of 2-propanol monomer were 90(4)% and 7×10^6 cm⁻³ in this deflected part of the molecular beam. The 45 fs laser-pulse ionization of 2-propanol with peak intensities of 3×10^{13} W/cm² and 7×10^{13} W/cm² was studied. The 2-propanol monomer

showed two fragmentation channels in the strong-field ionization process and the ratio of $M \rightarrow [M-CH_3]^+$ to $M \rightarrow [M-OH]^+$ was estimated to be ~ 5 . The fragmenting fractions of the monomer were estimated to be 83 % and 89 % at the lower and higher peak intensities, respectively. The produced intense, cold, and pure 2-propanol monomer beam is well-suited for further investigations, such as diffractive imaging [26, 46], chemical reaction [24] and combustion [47] studies.

ACKNOWLEDGMENTS

This work has been supported by the Clusters of Excellence “Center for Ultrafast Imaging” (CUI, EXC 1074, ID 194651731) and “Advanced Imaging of Matter” (AIM, EXC 2056, ID 390715994) of the Deutsche Forschungsgemeinschaft (DFG) and by the European Research Council under the European Union’s Seventh Framework Program (FP7/2007-2013) through the Consolidator Grant COMOTION (ERC-Küpper-614507). J.W. and L.H. acknowledge fellowships within the framework of the Helmholtz-OCPC postdoctoral exchange program and J.O. gratefully acknowledges a fellowship by the Alexander von Humboldt Foundation.

|| Permanent address: Department of Physics, Tsinghua University, 100084, Beijing, China

§ Permanent address: Institute of Atomic and Molecular Physics, Jilin University, Changchun 130012, China

‡ Present address: Department of Physics and Astronomy, University College London, Gower Street, London WC1E 6BT, UK

* Corresponding author. Email: jochen.kuepper@cfel.de; URL: <https://www.controlled-molecule-imaging.org>

- [1] A. V. Burenin, Rigorous description of an energy spectrum of the isopropanol molecule taking into account the internal rotation of methyl tops, *Opt. Spectrosc.* **120**, 848 (2016).
- [2] A. V. Burenin, A rigorous description of the energy spectrum of the isopropanol molecule taking into account the internal rotation of hydroxyl, *Opt. Spectrosc.* **120**, 854 (2016).
- [3] A. Maeda, I. R. Medvedev, F. C. D. Lucia, and E. Herbst, The millimeter- and submillimeter-wave spectrum of isopropanol $[(CH_3)_2CHOH]$, *Astrophys. J. Suppl. Ser.* **166**, 650 (2006).
- [4] J. García-Gavín, R. Lissens, A. Timmermans, and A. Goossens, Allergic contact dermatitis caused by isopropyl alcohol: a missed allergen?, *Contact Derm.* **65**, 101 (2011).
- [5] J. C. Dobrowolski, S. Ostrowski, R. Kołos, and M. H. Jamróz, Ar-matrix IR spectra of 2-propanol and its OD, D₇ and D₈ isotopologues, *Vib. Spectrosc.* **48**, 82 (2008).
- [6] C. Tanaka, Vibrational spectra of isopropyl alcohol and its deuterated species $(CH_3)_2CHOD$, $(CD_3)_2CHOH$, $(CD_3)_2CHOD$, *Nippon Kagaku Zasshi* **83**, 521 (1962).

- [7] S. Kondo and E. Hirota, Microwave spectrum and internal rotation of isopropyl alcohol, *J. Mol. Spectrosc.* **34**, 97 (1970).
- [8] E. Hirota, Internal rotation in isopropyl alcohol studied by microwave spectroscopy, *J. Phys. Chem.* **83**, 1457 (1979).
- [9] O. Ulenikov, A. Malikova, C. Qagar, S. Musaev, A. Adilov, and M. Mehtiev, On the analysis of the gauche-form microwave spectrum of the isopropyl alcohol molecule, *J. Mol. Spectrosc.* **145**, 262 (1991).
- [10] E. Hirota and Y. Kawashima, Internal rotation of the hydroxyl group in isopropanol and the chirality of the gauche form: Fourier transform microwave spectroscopy of $(\text{CH}_3)_2\text{CHOD}$, *J. Mol. Spectrosc.* **207**, 243 (2001).
- [11] G. Scoles, ed., *Atomic and molecular beam methods*, Vol. 1 & 2 (Oxford University Press, New York, NY, USA, 1988 & 1992).
- [12] M. Hillenkamp, S. Keinan, and U. Even, Condensation limited cooling in supersonic expansions, *J. Chem. Phys.* **118**, 8699 (2003).
- [13] T. Wang, T. Yang, C. Xiao, Z. Sun, D. Zhang, X. Yang, M. L. Weichman, and D. M. Neumark, Dynamical resonances in chemical reactions, *Chem. Soc. Rev.* **47**, 6744 (2018).
- [14] H. Schaal, T. Häber, and M. A. Suhm, Hydrogen bonding in 2-propanol. The effect of fluorination, *J. Phys. Chem. A* **104**, 265 (2000).
- [15] L. Evangelisti, Q. Gou, G. Feng, W. Caminati, G. J. Mead, I. A. Finneran, P. B. Carroll, and G. A. Blake, Conformational equilibrium and internal dynamics in the iso-propanol–water dimer, *Phys. Chem. Chem. Phys.* **19**, 568 (2017).
- [16] I. León, I. Usabiaga, J. Millán, E. J. Cocinero, A. Lesarri, and J. A. Fernández, Mimicking anesthetic–receptor interactions in jets: the propofol–isopropanol cluster, *Phys. Chem. Chem. Phys.* **16**, 16968 (2014).
- [17] C. Ng, Molecular beam photoionization studies of molecules and clusters, *Adv. Chem. Phys.*, 263 (1982).
- [18] R. E. Leckenby, E. J. Robbins, P. A. Trevalion, and B. H. Flowers, Condensation embryos in an expanding gas beam, *Proc. Royal Soc. London A* **280**, 409 (1964).
- [19] G. Fischer, R. E. Miller, P. F. Vohralik, and R. O. Watts, Molecular beam infrared spectra of dimers formed from acetylene, methyl acetylene, and ethene as a function of source pressure and concentration, *J. Chem. Phys.* **83**, 1471 (1985).
- [20] O. F. Hagen and W. Obert, Cluster formation in expanding supersonic jets: Effect of pressure, temperature, nozzle size, and test gas, *J. Chem. Phys.* **56**, 1793 (1972).
- [21] H. T. Jonkman, U. Even, and J. Kommandeur, Clusters of organic molecules in a supersonic jet expansion, *J. Phys. Chem.* **89**, 4240 (1985).
- [22] H. Haberland, A model for the processes happening in a rare-gas cluster after ionization, *Surf. Sci.* **156**, 305 (1985).
- [23] W. Schöllkopf and J. P. Toennies, Nondestructive mass selection of small van der Waals clusters, *Science* **266**, 1345 (1994).
- [24] Y.-P. Chang, K. Długołęcki, J. Küpper, D. Rösch, D. Wild, and S. Willitsch, Specific chemical reactivities of spatially separated 3-aminophenol conformers with cold Ca^+ ions, *Science* **342**, 98 (2013), arXiv:1308.6538 [physics].
- [25] A. Kilaj, H. Gao, D. Rösch, U. Rivero, J. Küpper, and S. Willitsch, Observation of different reactivities of para- and ortho-water towards trapped diazenylium ions, *Nat. Commun.* **9**, 2096 (2018).
- [26] J. Küpper, S. Stern, L. Holmegaard, F. Filsinger, A. Rouzée, A. Rudenko, P. Johnsson, A. V. Martin, M. Adolph, A. Aquila, S. Bajt, A. Barty, C. Bostedt, J. Bozek, C. Caleman, R. Coffee, N. Coppola, T. Delmas, S. Epp, B. Erk, L. Foucar, T. Gorkhover, L. Gumprecht, A. Hartmann, R. Hartmann, G. Hauser, P. Holl, A. Hömke, N. Kimmel, F. Krasniqi, K.-U. Kühnel, J. Maurer, M. Messerschmidt, R. Moshhammer, C. Reich, B. Rudek, R. Santra, I. Schlichting, C. Schmidt, S. Schorb, J. Schulz, H. Soltau, J. C. H. Spence, D. Starodub, L. Strüder, J. Thøgersen, M. J. J. Vrakking, G. Weidenspointner, T. A. White, C. Wunderer, G. Meijer, J. Ullrich, H. Stapelfeldt, D. Rolles, and H. N. Chapman, X-ray diffraction from isolated and strongly aligned gas-phase molecules with a free-electron laser, *Phys. Rev. Lett.* **112**, 083002 (2014), arXiv:1307.4577 [physics].
- [27] J. Yang, X. Zhu, T. J. A. Wolf, Z. Li, J. P. F. Nunes, R. Coffee, J. P. Cryan, M. Gühr, K. Hegazy, T. F. Heinz, K. Jobe, R. Li, X. Shen, T. Veccione, S. Weathersby, K. J. Wilkin, C. Yoneda, Q. Zheng, T. J. Martínez, M. Centurion, and X. Wang, Imaging CF_3I conical intersection and photodissociation dynamics with ultrafast electron diffraction, *Science* **361**, 64 (2018).
- [28] F. Filsinger, G. Meijer, H. Stapelfeldt, H. Chapman, and J. Küpper, State- and conformer-selected beams of aligned and oriented molecules for ultrafast diffraction studies, *Phys. Chem. Chem. Phys.* **13**, 2076 (2011), arXiv:1009.0871 [physics].
- [29] Y.-P. Chang, D. A. Horke, S. Trippel, and J. Küpper, Spatially-controlled complex molecules and their applications, *Int. Rev. Phys. Chem.* **34**, 557 (2015), arXiv:1505.05632 [physics].
- [30] S. Y. T. van de Meerakker, H. L. Bethlem, N. Vanhaecke, and G. Meijer, Manipulation and control of molecular beams, *Chem. Rev.* **112**, 4828 (2012).
- [31] F. Filsinger, J. Küpper, G. Meijer, L. Holmegaard, J. H. Nielsen, I. Nevo, J. L. Hansen, and H. Stapelfeldt, Quantum-state selection, alignment, and orientation of large molecules using static electric and laser fields, *J. Chem. Phys.* **131**, 064309 (2009), arXiv:0903.5413 [physics].
- [32] J. H. Nielsen, P. Simesen, C. Z. Bisgaard, H. Stapelfeldt, F. Filsinger, B. Friedrich, G. Meijer, and J. Küpper, Stark-selected beam of ground-state OCS molecules characterized by revivals of impulsive alignment, *Phys. Chem. Chem. Phys.* **13**, 18971 (2011), arXiv:1105.2413 [physics].
- [33] D. A. Horke, Y.-P. Chang, K. Długołęcki, and J. Küpper, Separating para and ortho water, *Angew. Chem. Int. Ed.* **53**, 11965 (2014), arXiv:1407.2056 [physics].
- [34] F. Filsinger, U. Erlekam, G. von Helden, J. Küpper, and G. Meijer, Selector for structural isomers of neutral molecules, *Phys. Rev. Lett.* **100**, 133003 (2008), arXiv:0802.2795 [physics].
- [35] T. Kierspel, D. A. Horke, Y.-P. Chang, and J. Küpper, Spatially separated polar samples of the *cis* and *trans* conformers of 3-fluorophenol, *Chem. Phys. Lett.* **591**, 130 (2014), arXiv:1312.4417 [physics].
- [36] S. Trippel, Y.-P. Chang, S. Stern, T. Mullins, L. Holmegaard, and J. Küpper, Spatial separation of state- and size-selected neutral clusters, *Phys. Rev. A* **86**, 033202 (2012), arXiv:1208.4935 [physics].
- [37] N. Teschmit, D. A. Horke, and J. Küpper, Spatially separating the conformers of a dipeptide, *Angew. Chem. Int.*

- Ed. **57**, 13775 (2018), arXiv:1805.12396 [physics].
- [38] H. S. You, J. Kim, S. Han, D.-S. Ahn, J. S. Lim, and S. K. Kim, Spatial isolation of conformational isomers of hydroquinone and its water cluster using the stark deflector, *J. Phys. Chem. A* **122**, 1194 (2018).
 - [39] M. Johny, J. Onvlee, T. Kierspel, H. Bieker, S. Trippel, and J. Küpper, Spatial separation of pyrrole and pyrrole-water clusters, *Chem. Phys. Lett.* **721**, 149–152 (2019), arXiv:1901.05267 [physics].
 - [40] H. Bieker, J. Onvlee, M. Johny, L. He, T. Kierspel, S. Trippel, D. A. Horke, and J. Küpper, Pure molecular beam of water dimer, *J. Phys. Chem. A* **123**, 7486 (2019), arXiv:1904.08716 [physics].
 - [41] D. Irímia, D. Dobrikov, R. Kortekaas, H. Voet, D. A. van den Ende, W. A. Groen, and M. H. M. Janssen, A short pulse (7 μ s FWHM) and high repetition rate (dc–5kHz) cantilever piezovalve for pulsed atomic and molecular beams, *Rev. Sci. Instrum.* **80**, 113303 (2009).
 - [42] J. S. Kienitz, S. Trippel, T. Mullins, K. Długołęcki, R. González-Férez, and J. Küpper, Adiabatic mixed-field orientation of ground-state-selected carbonyl sulfide molecules, *Chem. Phys. Chem.* **17**, 3740 (2016), arXiv:1607.05615 [physics].
 - [43] S. Trippel, T. Mullins, N. L. M. Müller, J. S. Kienitz, K. Długołęcki, and J. Küpper, Strongly aligned and oriented molecular samples at a kHz repetition rate, *Mol. Phys.* **111**, 1738 (2013), arXiv:1301.1826 [physics].
 - [44] R. S. Ruoff, T. D. Klots, T. Emilsson, and H. S. Gutowsky, Relaxation of conformers and isomers in seeded supersonic jets of inert gases, *J. Chem. Phys.* **93**, 3142 (1990).
 - [45] Y.-P. Chang, F. Filsinger, B. Sartakov, and J. Küpper, CMISTARK: Python package for the stark-effect calculation and symmetry classification of linear, symmetric and asymmetric top wavefunctions in dc electric fields, *Comp. Phys. Comm.* **185**, 339 (2014), arXiv:1308.4076 [physics].
 - [46] A. Barty, J. Küpper, and H. N. Chapman, Molecular imaging using x-ray free-electron lasers, *Annu. Rev. Phys. Chem.* **64**, 415 (2013).
 - [47] C. Esarte, M. Abián, Á. Millera, R. Bilbao, and M. U. Alzueta, Gas and soot products formed in the pyrolysis of acetylene mixed with methanol, ethanol, isopropanol or n-butanol, *Energy* **43**, 37 (2012).